Opposing roles of TGFβ and BMP signaling in prostate cancer development

Xin Lu,[1,2,3,8] Eun-Jung Jin,[1,4,8] Xi Cheng,[2,5] Shan Feng,[2,6] Xiaoying Shang,[1] Pingna Deng,[1] Shan Jiang,[7] Qing Chang,[7] Sharif Rahmy,[2] Seema Chaudhary,[2] Xuemin Lu,[2] Ren Zhao,[5] Y. Alan Wang,[1] and Ronald A. DePinho[1]

[1]Department of Cancer Biology, The University of Texas MD Anderson Cancer Center, Houston, Texas 77054, USA; [2]Department of Biological Sciences, Boler-Parseghian Center for Rare and Neglected Diseases, Harper Cancer Research Institute, University of Notre Dame, Notre Dame, Indiana 46556, USA; [3]Tumor Microenvironment and Metastasis Program, Indiana University Melvin and Bren Simon Cancer Center, Indianapolis, Indiana 46202, USA; [4]Department of Biological Science, Wonkwang University, Cheonbuk, Iksan 570-749, South Korea; [5]Department of General Surgery, Ruijin Hospital, Shanghai Jiao Tong University School of Medicine, Shanghai 200025, China; [6]School of Life Sciences, Tsinghua University, Beijing 100084, China; [7]Institute for Applied Cancer Science, The University of Texas MD Anderson Cancer Center, Houston, Texas 77054, USA

SMAD4 constrains progression of *Pten*-null prostate cancer and serves as a common downstream node of transforming growth factor β (TGFβ) and bone morphogenetic protein (BMP) pathways. Here, we dissected the roles of TGFβ receptor II (TGFBR2) and BMP receptor II (BMPR2) using a *Pten*-null prostate cancer model. These studies demonstrated that the molecular actions of TGFBR2 result in both SMAD4-dependent constraint of proliferation and SMAD4-independent activation of apoptosis. In contrast, BMPR2 deletion extended survival relative to *Pten* deletion alone, establishing its promoting role in BMP6-driven prostate cancer progression. These analyses reveal the complexity of TGFβ–BMP signaling and illuminate potential therapeutic targets for prostate cancer.

Supplemental material is available for this article.

Received September 12, 2017; revised version accepted December 4, 2017.

Prostate cancer (PCa) is the most commonly diagnosed malignancy and the third leading cause of cancer mortality in American men. PCa initiation and progression are governed by numerous genetic alterations (Shen and Abate-Shen 2010). Loss of the tumor suppressor *PTEN* is a common genetic aberration (Abeshouse et al. 2015; Robinson et al. 2015). Correspondingly, prostate-specific *Pten* deletion in mice produces slowly progressing prostate intraepithelial neoplasia (PIN), which, following a long latency, can progress to high-grade adenocarcinoma with minimal invasive and metastatic potential (Trotman et al. 2003; Wang et al. 2003). This slowly progressive disease results from the activation of a senescence program that can be neutralized by deletion of tumor suppressor genes *p53* (Chen et al. 2005) or *Smad4* (Ding et al. 2011). Of relevance to the present study, prostate-specific deletion of *Pten* and *Smad4* generates rapidly progressive PCa with metastasis to lymph nodes and the lungs (Ding et al. 2011; Wang et al. 2016).

The cross-talk between transforming growth factor β (TGFβ) and bone morphogenetic protein (BMP) signaling plays critical roles in a number of processes of organogenesis and homeostasis, with the output (antagonistic or synergistic) being highly context-dependent (McDonnell et al. 2001; Lu et al. 2010; Keller et al. 2011; Li et al. 2015). In cancer, the TGFβ pathway has long been recognized to exert opposing roles throughout cancer progression, switching from anti-tumor to prometastasis mechanisms depending on cell type and associated genetic alterations, among other factors (Massagué 2008). In PCa, inactivation the TGFβ pathway through deletion of *TGFβ receptor II* (*Tgfbr2*) can promote AKT-mediated PCa tumorigenesis (Bjerke et al. 2014), whereas enhanced TGFβ signaling can induce a pro-bone metastasis program (Fournier et al. 2015). Adding to the complexity, TGFβ-regulated responses can be mediated by several SMAD-independent pathways, best illustrated by TGFβ-induced activation of JNK and p38 MAPK to trigger apoptosis (Zhang 2009). With respect to BMP signaling, various BMP ligands can exert differential biological impacts on PCa tumorigenesis. For example, BMP6, which is overexpressed in some human PCa cases, has been shown to promote migration and invasion (Darby et al. 2008) and stimulate PCa growth and resistance to androgen receptor (AR) antagonists (Kwon et al. 2014). In contrast, BMP7 inhibits PCa cell proliferation (Kobayashi et al. 2011), although experimental evidence also supports an anti-apoptotic role (Yang et al. 2005). Moreover, in breast cancer, organ-specific bioavailability of BMP ligands and their antagonist, Coco, can dictate the efficiency of metastasis (Gao et al. 2012).

The importance of SMAD4 in PCa progression and the role of SMAD4 as the only common partner (co-SMAD) for all R-SMADs signaling from specific upstream receptors (Massagué 2008) prompted us to explore the relative contributions of TGFβ and BMP pathways. We explored the biological complexity of TGFβ and BMP signaling by genetic deletion of *Tgfbr2* and *BMP receptor II* (*Bmpr2*) in the context of the *Pten*-null PCa mouse model.

[*Keywords*: PTEN; SMAD4; TGFBR2; BMPR2; prostate cancer; bone metastasis]

[8]These authors contributed equally to this work.
Corresponding authors: rdepinho@mdanderson.org, yalanwang@mdanderson.org

Article is online at http://www.genesdev.org/cgi/doi/10.1101/gad.307116.117.

Results and Discussion

TGFBR2 is a more potent tumor suppressor than SMAD4 in PTEN-null PCa

Our previous work showed no discernable histological impact on the mouse prostate upon *Smad4* deletion using the prostate-specific Cre transgene (PB-Cre4) (Ding et al. 2011). Similarly, PB-Cre4-directed deletion of *Tgfbr2* (Chytil et al. 2002) or *Bmpr2* (Beppu et al. 2005) yielded no histological abnormalities over an observation period of 9 mo (Supplemental Fig. S1A). In each model, specific receptor expression loss was confirmed by immunohistochemistry (IHC) (Supplemental Fig. S1B,C). To compare more precisely the relative impact of SMAD4, TGFBR2, and BMPR2 deletion on the progression of the *Pten*-null PCa model, we generated the following cohorts and determined their median survival: *PB-Cre*$^+$ *Pten*$^{L/L}$ (55 wk), *PB-Cre*$^+$ *Pten*$^{L/L}$ *Smad4*$^{L/L}$ (16.4 wk), *PB-Cre*$^+$ *Pten*$^{L/L}$ *Tgfbr2*$^{L/L}$ (12.7 wk), and *PB-Cre*$^+$ *Pten*$^{L/L}$ *Bmpr2*$^{L/L}$ (73.6 wk) (Fig. 1A). These strikingly different outcomes imply that despite convergence on the SMAD4 node, TGFBR2 and BMPR2 exert opposing actions on PCa development. We also performed expression characterizations of some key proteins, including TGFBR2 and BMPR2 levels, which are comparable in wild-type prostates and *PB-Cre*$^+$ *Pten*$^{L/L}$ tumors (Supplemental Fig. S1B,C). In addition, AR expression among the prostate epithelial cells displayed modest variations in each of the four models compared with wild-type prostates, yet overall loss of *Tgrbr2* or *Bmpr2* in *PB-Cre*$^+$ *Pten*$^{L/L}$ tumors did not impact AR expression in any specific direction (Supplemental Fig. S2A). As expected, *Pten* loss resulted in increased phospho-AKT signal, which was not further impacted by the additional deletion of *Smad4*, *Tgfbr2*, or *Bmpr2* (Supplemental Fig. S2B,C). Based on the dramatic differences in the rate of tumor progression, we focused on addressing two key questions: how TGFBR2 displays stronger tumor-suppressive function than SMAD4 in prostate by comparing *PB-Cre*$^+$ *Pten*$^{L/L}$ *Smad4*$^{L/L}$ and *PB-Cre*$^+$ *Pten*$^{L/L}$ *Tgfbr2*$^{L/L}$ models and how BMPR2 promotes *Pten*-deficient prostate tumors by comparing *PB-Cre*$^+$ *Pten*$^{L/L}$ and *PB-Cre*$^+$ *Pten*$^{L/L}$ *Bmpr2*$^{L/L}$ models.

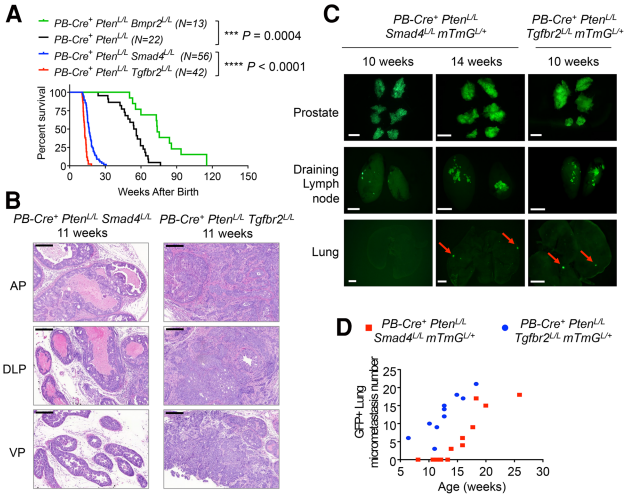

Figure 1. TGFBR2 is a more potent tumor suppressor than SMAD4. (*A*) Kaplan-Meier curve showing the survival of mice with the indicated genotypes and mouse numbers. The *P*-value was calculated using log-rank test. (*B*) H&E staining of the anterior prostate (AP), dorsolateral prostate (DLP), and ventral prostate (VP). Bar, 200 µm. (*C*) Fluorescence images of the indicated organs. Bars: prostate, 5 mm; lymph nodes, 1 mm; lungs, 2 mm. (*D*) Quantification of GFP$^+$ lung micrometastases of the two mTmG models at different ages.

Compared with *PB-Cre*$^+$ *Pten*$^{L/L}$ mice, both *PB-Cre*$^+$ *Pten*$^{L/L}$ *Smad4*$^{L/L}$ and *PB-Cre*$^+$ *Pten*$^{L/L}$ *Tgfbr2*$^{L/L}$ showed more aggressive tumor progression but at different rates. Therefore, we compared these two models. At 11 wk of age, most *PB-Cre*$^+$ *Pten*$^{L/L}$ *Smad4*$^{L/L}$ tumors presented with high-grade PIN, whereas *PB-Cre*$^+$ *Pten*$^{L/L}$ *Tgfbr2*$^{L/L}$ tumors progressed to adenocarcinoma with local invasion (Fig. 1B). Next, we compared the impact of TGFBR2 versus SMAD4 deficiencies on metastasis. To that end, the two models incorporated the fluorescence reporter *mTmG* (Muzumdar et al. 2007), which allows for Cre-dependent GFP expression in prostate epithelia cells. In the *PB-Cre*$^+$ *Pten*$^{L/L}$ *Smad4*$^{L/L}$ *mTmG*$^{L/+}$ model, GFP$^+$ PCa cells were detected in the draining lymph nodes as early as 10 wk of age and in the lungs as early as 14 wk of age (Fig. 1C). In comparison, the *PB-Cre*$^+$ *Pten*$^{L/L}$ *Tgfbr2*$^{L/L}$ *mTmG*$^{L/+}$ model showed disseminated neoplastic cells to the lymph nodes and the lungs as early as 6 wk of age (Supplemental Fig. S3A) and exhibited metastases in the lymph nodes and micrometastases in the lungs at full penetrance by 10 wk of age (Fig. 1C). In both models, there is a trend of age-dependent increase of lung micrometastasis, as enumerated by GFP signals (Fig. 1D). Moreover, it is intriguing to note that GFP$^+$ disseminated cancer cells are observed in mice with high-grade PIN, consistent with early dissemination mechanisms; these murine findings are consistent with the presence of disseminated disease in men with clinically localized PCa (Wood et al. 1994). The distant metastases in the lungs were stained positive for GFP, E-cadherin, AR, and phospho-AKT, validating their prostate origin and epithelial nature (Supplemental Fig. S3B). PCR genotyping of the *Pten* allele of microdissected lung metastases from both models further verified the loss of *Pten* (Supplemental Fig. S3C). Together, these findings indicate that TGFBR2 functions as a more potent tumor suppressor than SMAD4 in the progression of *Pten*-null PCa, including metastasis.

In *Pten*-null PCa, *Smad4* deletion results in a dramatic increase in cell proliferation due to up-regulation of cyclin D1, which is normally transcriptionally repressed by SMAD4 in this model; in contrast, no change in the rate of apoptosis was observed as a function of SMAD4 status (Ding et al. 2011). We thus compared the tumor biological impact of SMAD4 and TGFBR2 in the *Pten*-null PCa model with respect to proliferation (Ki67), apoptosis (cleaved caspase 3 [CC3]), and cyclin D1 levels (Fig. 2A–C). While cancer cells in both genotypes showed comparable Ki67 and cyclin D1 staining, cancer cells in the *PB-Cre*$^+$ *Pten*$^{L/L}$ *Tgfbr2*$^{L/L}$ tumors exhibited significantly lower CC3 staining. The comparable proliferation yet reduced apoptosis observed in *PB-Cre*$^+$ *Pten*$^{L/L}$ *Tgfbr2*$^{L/L}$ tumors as compared with *PB-Cre*$^+$ *Pten*$^{L/L}$ *Smad4*$^{L/L}$ tumors was intriguing, as previous work has shown that TGFβ can activate JNK and p38 MAPK kinase pathways through SMAD-independent mechanisms to induce apoptosis (Zhang 2009). Indeed, comparison of JNK, p38 MAPK, and ERK activation in these two models at 10 wk of age revealed no differences in phospho-JNK and phospho-Erk signals (Supplemental Fig. S3D) but did show lower phospho-p38 MAPK signal in *PB-Cre*$^+$ *Pten*$^{L/L}$ *Tgfbr2*$^{L/L}$ tumors relative to *PB-Cre*$^+$ *Pten*$^{L/L}$ *Smad4*$^{L/L}$ tumors

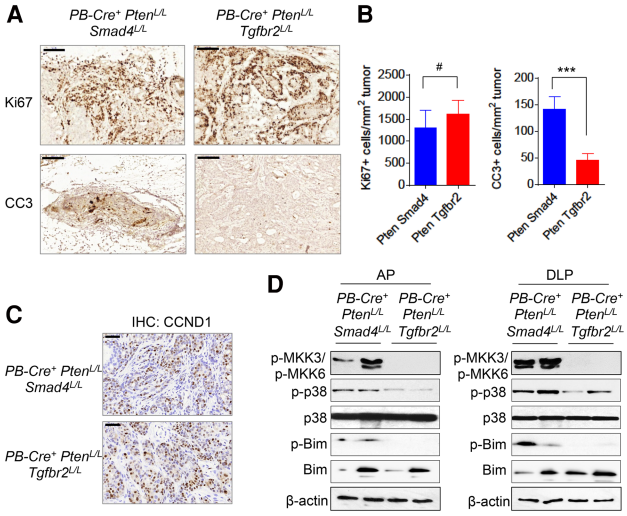

Figure 2. TGFβ signaling restricts PCa partly through the SMAD-independent apoptosis pathway. (*A*) IHC staining of Ki67 and CC3 in tumors from 11-wk-old mice with the indicated genotypes. Bar, 100 µm. (*B*) Quantification of the Ki67 and CC3 IHC staining. $n = 4$. Data represent mean ± SD. (***) $P < 0.001$; (#) $P > 0.05$, Student's *t*-test. (*C*) IHC staining of cyclin D1 (CCND1) for tumors from 15-wk-old mice with the indicated genotypes. Bar, 50 µm. (*D*) Western blot of phospho-p38, total p38, phospho-Bim, and total Bim for tumors from 10-wk-old mice with the indicated genotypes.

(Fig. 2D). TGFβ-dependent activation of p38 MAPK is known to be mediated by MAPK kinases such as MKK3/6 (Zhang 2009), and activated p38 can further phosphorylate the apoptosis effector Bim (Cai et al. 2006), prompting us to compare phospho-MKK3/6 and phospho-Bim levels. *PB-Cre*$^+$ *Pten*$^{L/L}$ *Tgfbr2*$^{L/L}$ tumors exhibit lower phospho-MKK3/6 and phospho-Bim signals relative to *PB-Cre*$^+$ *Pten*$^{L/L}$ *Smad4*$^{L/L}$ (Fig. 2D; Supplemental Fig. S3E). Together, these data support a model in which attenuated MKK3/6–p38 MAPK–Bim signaling and consequent reduction of apoptosis contribute to the increased aggressiveness of *PB-Cre*$^+$ *Pten*$^{L/L}$ *Tgfbr2*$^{L/L}$ tumors relative to *PB-Cre*$^+$ *Pten*$^{L/L}$ *Smad4*$^{L/L}$ tumors.

TGFBR2 loss enhances PCa seeding and outgrowth in the bone

In human PCa, the bone is the most common site for distant metastasis, prompting comparison of bone metastasis potential in our models. As noted above, *PB-Cre*$^+$ *Pten*$^{L/L}$ *Tgfbr2*$^{L/L}$ *mTmG*$^{L/+}$ mice disseminate GFP$^+$ tumor cells to the lymph nodes and the lungs at a younger age relative to *PB-Cre*$^+$ *Pten*$^{L/L}$ *Smad4*$^{L/L}$ *mTmG*$^{L/+}$ mice (Fig. 1D). Over the entire mouse life span in these two models, there was no development of overt bone metastasis, although occasional GFP$^+$ disseminated tumor cells (DTCs) were present in femoral and tibial bone marrow of late stage *PB-Cre*$^+$ *Pten*$^{L/L}$ *Tgfbr2*$^{L/L}$ *mTmG*$^{L/+}$ and *PB-Cre*$^+$ *Pten*$^{L/L}$ *Smad4*$^{L/L}$ *mTmG*$^{L/+}$ mice (Supplemental Fig. S4A). PCR genotyping of the *Pten* allele was used to confirm the presence of the DTCs, demonstrating that pooled femoral and tibial bone marrow from the two models exhibited DTCs as early as 3 mo of age in the *PB-Cre*$^+$ *Pten*$^{L/L}$ *Tgfbr2*$^{L/L}$ mice as opposed to 5 mo of age in the *PB-Cre*$^+$ *Pten*$^{L/L}$ *Smad4*$^{L/L}$ mice (Supplemental Fig. S4B,C).

In a spontaneous tumor model, differences in metastatic kinetics may be the consequence of differences in primary tumor growth. To study metastatic colonization directly, we performed the experimental bone metastasis assay by intratibial inoculation of the same number of primary cancer cells from *PB-Cre*$^+$ *Pten*$^{L/L}$ *Tgfbr2*$^{L/L}$ *mTmG*$^{L/+}$ and *PB-Cre*$^+$ *Pten*$^{L/L}$ *Smad4*$^{L/L}$ *mTmG*$^{L/+}$ mice (Fig. 3A). This assay demonstrated greater bone metastatic burden and reduced survival of mice injected with *PB-Cre*$^+$ *Pten*$^{L/L}$ *Tgfbr2*$^{L/L}$ *mTmG*$^{L/+}$ PCa cells relative to those injected with *PB-Cre*$^+$ *Pten*$^{L/L}$ *Smad4*$^{L/L}$ *mTmG*$^{L/+}$ cells (Fig. 3B–D; Supplemental Fig. S4D). Thus, in this experimental system, elimination of TGFBR2 provokes increased metastatic growth potential in the bone microenvironment relative to elimination of SMAD4. It is important to note, however, that these results also underscore that multiple additional genetic events are likely needed to promote spontaneous metastasis to the bone in mice, as noted previously (Ding et al. 2012).

The BMP pathway promotes Pten-deficient primary PCa development

Consistent with the longer survival of *PB-Cre*$^+$ *Pten*$^{L/L}$ *Bmpr2*$^{L/L}$ mice relative to *PB-Cre*$^+$ *Pten*$^{L/L}$ mice, magnetic resonance imaging (MRI) and histological analysis documented slower tumor growth and more benign pathology in the *PB-Cre*$^+$ *Pten*$^{L/L}$ *Bmpr2*$^{L/L}$ mice compared with age-matched *PB-Cre*$^+$ *Pten*$^{L/L}$ controls (Fig. 4A,B). Consistent with this slower growth rate, *PB-Cre*$^+$ *Pten*$^{L/L}$ *Bmpr2*$^{L/L}$ prostate tumors contained decreased numbers of Ki67$^+$ proliferating cells compared with *PB-Cre*$^+$ *Pten*$^{L/L}$ tumors in mice of 3–4 mo of age (Supplemental Fig. S5A,B), yet both genotypes displayed comparable levels of apoptosis (Supplemental Fig. S5A,B). As these

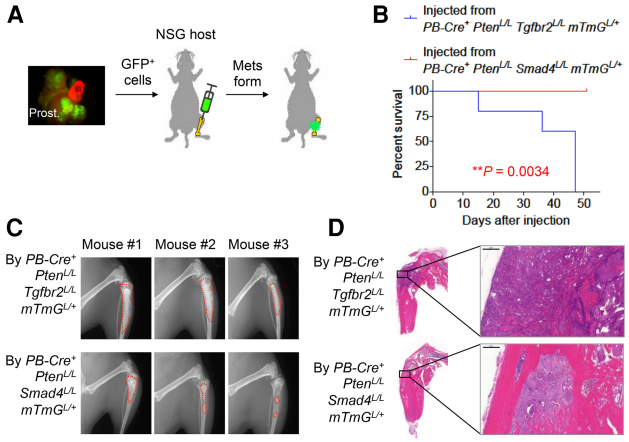

Figure 3. TGFBR2 loss enhances PCa seeding and outgrowth in the bone. (*A*) Schematic illustration of the experimental bone metastasis procedure. GFP$^+$ cells were isolated using FACS. (*B*) Survival curve of NSG mice injected with primary cells isolated from 11-wk-old mice with the indicated genotypes. $n = 5$. *P*-value was calculated by log-rank test. (*C*) X-ray images of the long bones of three representative mice injected with PCa cells of the indicated genotypes. Bone area demarcated with red dotted line indicates bone lesions. (*D*) Representative H&E staining at low and high magnification to show the metastasis burden in mice injected with primary cells isolated from mice of the indicated genotypes. Bar, 200 µm.

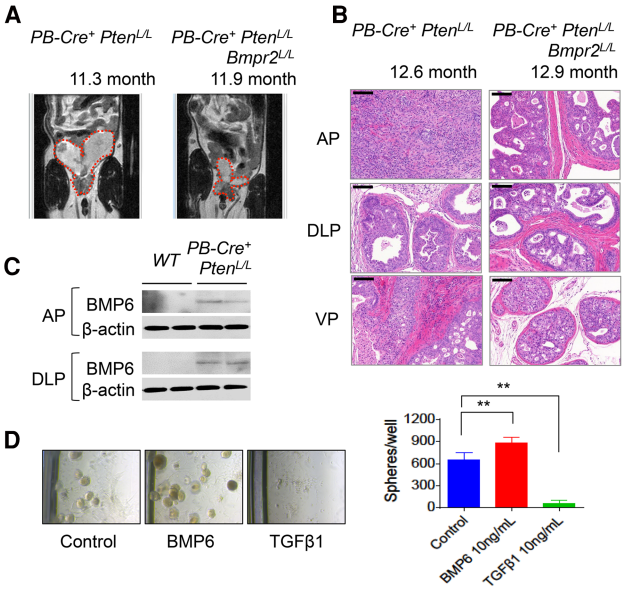

Figure 4. BMPR2 deletion delays PCa progression and prolongs mouse survival. (*A*) Representative MRI images of mice of the indicated genotypes and ages, with prostate outlined by a red contour. (*B*) H&E staining of the anterior prostate (AP), dorsolateral prostate (DLP), and ventral prostate (VP). Bar, 200 µm. (*C*) Western blot of BMP6 and β-actin for the anterior prostate and dorsolateral prostate of wild type (WT) and *PB-Cre*$^{+}$ *Pten*$^{L/L}$ prostates. (*D*) Sphere formation assay using primary tumor cells isolated from *PB-Cre*$^{+}$ *Pten*$^{L/L}$ prostates and treated with BMP6 or TGFβ1. $n = 4$. Data represent mean ± SD. (**) $P < 0.01$, Student's *t*-test.

findings support a role for BMPR2 signaling in promoting PCa progression, we next explored the role of some of its ligands with known links to PCa biology. While BMP2, BMP4, and BMP7 were undetectable by Western blot analysis in wild-type and *PB-Cre*$^{+}$ *Pten*$^{L/L}$ prostates (data not shown), BMP6 was expressed at higher levels in *PB-Cre*$^{+}$ *Pten*$^{L/L}$ prostates compared with wild-type prostates (Fig. 4C). These murine observations align with human PCa studies showing elevated BMP6 levels in the transition from prostate hyperplasia to PCa as well as a correlation of BMP6 expression with higher Gleason scores (Barnes et al. 1995; Yuen et al. 2008). Thus, to secure validation of a role for BMP6 in PCa cell proliferation in our genetic model, primary PCa cells derived from *PB-Cre*$^{+}$ *Pten*$^{L/L}$ mice were examined in the prostatosphere assay in the presence of BMP6 or TGFβ1. Sphere-forming ability was significantly increased with BMP6 treatment yet almost completely blocked upon TGFβ1 treatment (Fig. 4D). On the other hand, primary PCa cells derived from *PB-Cre*$^{+}$ *Pten*$^{L/L}$ *Bmpr2*$^{L/L}$ mice failed to respond to BMP6 (Supplemental Fig. S5C), demonstrating the essential role of BMPR2 in mediating the BMP6 effect in our model. We also obtained equivalent results with BMP6 and TGFβ1 in the organoid culture method (Supplemental Fig. S5D), which better preserves luminal cell representation in the formed spheres (Chua et al. 2014).

To better understand BMP pathway function in PCa progression, we profiled the transcriptome of 6-mo-old *PB-Cre*$^{+}$ *Pten*$^{L/L}$ and *PB-Cre*$^{+}$ *Pten*$^{L/L}$ *Bmpr2*$^{L/L}$ tumors (anterior prostate) using RNA sequencing and detected 361 differentially expressed genes (Fig. 5A; Supplemental Table S1). Ingenuity Pathway Analysis (IPA) of the most up-regulated genes in *PB-Cre*$^{+}$ *Pten*$^{L/L}$ tumors compared with *PB-Cre*$^{+}$ *Pten*$^{L/L}$ *Bmpr2*$^{L/L}$ tumors showed "role of osteoblasts, osteoclasts, and chondrocytes in rheumatoid arthritis" as the top pathway (P-value = 2.89×10^{-6}) (Supplemental Fig. S5E; Supplemental Table S2), a finding consistent with the classical function of the BMP pathway in bone cell homeostasis. As a consequence of BMPR2 loss, the top-ranked putative master regulator (accounting for differential gene expression based on the causal network algorithm in IPA) was BMP2 (P-value = 1.43×10^{-15}), which is an in silico representative of the BMP ligands. In addition, the canonical BMP pathway was predicted to be inhibited in *PB-Cre*$^{+}$ *Pten*$^{L/L}$ *Bmpr2*$^{L/L}$ tumors (Fig. 5B; Supplemental Table S3). Interestingly, inhibition of lipopolysaccharide-regulated genes was identified as a top transcriptomic alteration in the *Bmpr2* knockout (P-value = 1.46×10^{-8}) using the upstream regulator analysis in IPA (Fig. 5C). This was because a number of important inflammation-related pathways mediated by central signaling regulators, including NFκB and STAT3, were predicted

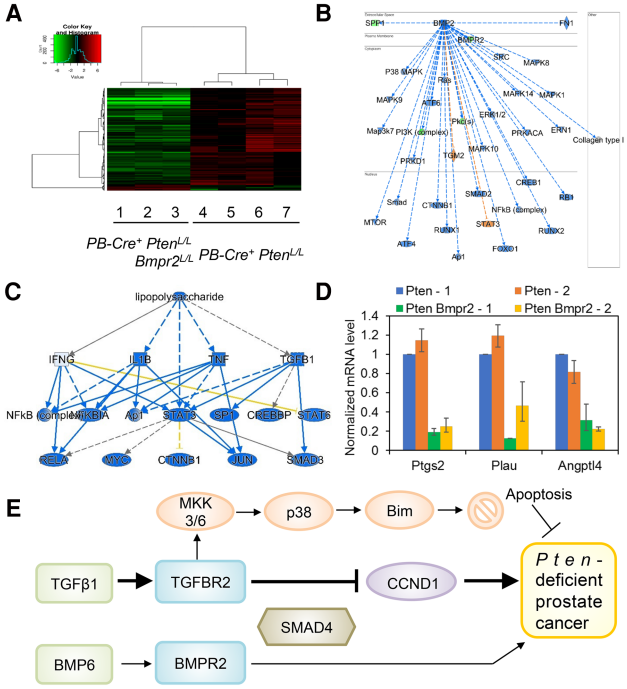

Figure 5. The BMP pathway promotes primary PCa progression. (*A*) Hierarchical clustering of differentially expressed genes from prostate tumors of 5-mo-old *PB-Cre*$^{+}$ *Pten*$^{L/L}$ and *PB-Cre*$^{+}$ *Pten*$^{L/L}$ *Bmpr2*$^{L/L}$ mice. (*B*) Causal network of the top master regulator BMP2 generated by IPA. The overwhelmingly blue colors of the connections and gene icons indicate that the canonical BMP pathway is predicted to be inhibited in *PB-Cre*$^{+}$ *Pten*$^{L/L}$ *Bmpr2*$^{L/L}$ tumors, consistent with the activation *z*-score being −4.273. (*C*) Mechanistic network view showing that the downstream pathways of lipopolysaccharide (i.e., inflammation related) are broadly inhibited in *PB-Cre*$^{+}$ *Pten*$^{L/L}$ *Bmpr2*$^{L/L}$ tumors. The graph was generated by IPA. (*D*) Differential expression of *Ptgs2*, *Plau*, and *Angptl4* between the two models, validated using qRT–PCR with two biological replicates and three technical replicates. (*E*) Model depicting the antagonistic roles of the TGFβ and BMP pathways (converged on SMAD4) in *Pten*-deficient PCa progression.

to be inhibited in *PB-Cre*$^{+}$ *Pten*$^{L/L}$ *Bmpr2*$^{L/L}$ tumors, based on significant down-regulation of many downstream genes of these regulators (Supplemental Table S4). Some prominent down-regulated genes include *prostaglandin-endoperoxide synthase 2* (*Ptgs2* [also known as *cyclooxygenase-2*], down by 12.6-fold), *urokinase plasminogen activator* (*Plau* [also known as *uPA*], down by 8.1-fold), and *angiopoietin-like 4* (*Angptl4*, down by 3.8-fold). The differential expression of these genes was validated by quantitative RT–PCR (qRT–PCR) (Fig. 5D). These results suggest that the protumor effect from BMP signaling in *Pten*-deficient tumors is likely through canonical BMP signaling targets as well as targets regulated by BMP signaling with its emerging role in inflammation (Ye et al. 2015; Nguyen et al. 2017). Additional genetic and molecular studies will be needed to define the role of these gene networks in BMP signaling in *Pten*-null PCa.

In summary, this study documents the opposing roles of the TGFβ and BMP pathways in PCa development in the context of *Pten* deficiency. We show that the TGFβ pathway suppresses PCa development through SMAD4-dependent and SMAD4-independent mechanisms, whereas BMP signaling promotes PCa progression likely through both canonical BMP targets and promotion of inflammation (Fig. 5E). When both pathways are intact, we propose that the net effect on tumor suppression reflects a dominant role of TGFβ over BMP signaling. Antagonistic interactions between the TGFβ and BMP pathways have been reported in processes such as chondrogenesis (Keller et al. 2011), kidney fibrosis (Scherner et al. 2007), and keratinocyte differentiation (McDonnell et al. 2001). Our genetic study reveals the antagonistic cross-talk of the two pathways in cancer. We stress that the activity of either TGFβ or BMP signaling in PCa progression depends on the genetic and environmental context of PCa cells as well as the stage of the disease. The TGFβ pathway suppresses primary and metastatic PCa progression in the autochthonous *Pten* deletion model, as shown by us and others (Bjerke et al. 2014). Meanwhile, TGFβ has been shown to promote bone metastasis of PCa in immunodeficient models (Fournier et al. 2015), suggesting that the status of other genes (e.g., PTEN and PMEPA1) may determine the outcome of TGFβ signaling. For BMP signaling, the specific ligands can dictate the biological effect because, while BMP6 (Fig. 4D) and BMP4 (Lee et al. 2011; Lin et al. 2017) promote PCa growth in either a cell-autonomous or a non-cell-autonomous manner, BMP7 (not detected in *PB-Cre*$^{+}$ *Pten*$^{L/L}$ tumors) inhibits PCa growth (Kobayashi et al. 2011). The connection of BMP signaling with genes regulating inflammation is of particular interest. *PB-Cre*$^{+}$ *Pten*$^{L/L}$ prostate tumors are infiltrated by myeloid-derived suppressor cells (MDSCs) (Garcia et al. 2014). In addition, a few genes down-regulated in *PB-Cre*$^{+}$ *Pten*$^{L/L}$ *Bmpr2*$^{L/L}$ tumors (e.g., *Ptgs2* and *Plau*) encode proteins responsible for MDSC recruitment (Fujita et al. 2011; Ilkovitch et al. 2012). Therefore, it will be important for future studies to investigate whether BMP signaling regulates infiltration and function of MDSCs and other immune cells in PCa. The finding that ablation of BMP signaling via BMPR2 extinction in *Pten*-deficient PCa cells significantly prolongs mouse survival could have important translational implications, as it suggests that the BMP pathway may be a therapeutic target to extend overall survival in a large percentage of PCa patients.

Materials and methods

Mouse strains

The *PB-Cre*$^{+}$ *Pten*$^{L/L}$ *Smad4*$^{L/L}$ model was developed previously (Ding et al. 2011) and backcrossed to the C57BL/6 background for more than four generations. *B6.129S6-Tgfbr2*^{tm1Hlm}*/N* strain was from the National Cancer Institute Mouse Repository. The *B6.129S4(Cg)-Bmpr2*$^{tm1.1Enl}$*/Mmnc* strain was from the Mutant Mouse Resource and Research Centers. mTmG and NSG mice were purchased from Jackson Laboratory. Mice were maintained in pathogen-free conditions at MD Anderson Cancer Center. For survival curves, the mice were examined daily, and all mice with excessive prostate tumor size and moribund signs, including obstruction of urination, were euthanized in compliance with our animal protocol and considered positive values for survival curves. All manipulations were approved under the MD Anderson Cancer Center Institutional Animal Care and Use Committee.

Additional experimental details are in the Supplemental Material.

Acknowledgments

We thank Kun Zhao, Zhaohui Xu, and Zhuangna Fang for animal husbandry; Di Zhao for help with the RNA sequencing experiment; Filippo Giancotti for helpful suggestions on the study and manuscript writing; Denise Spring and Sam Arroyo for editing the manuscript; and all members of the DePinho laboratory for a variety of technical support and helpful suggestions. The project was supported by R01 CA084628 (R.A.D.), P01CA117969 (R.A.D.), and the Clayton and Modesta Williams Cancer Research Fund (R.A.D.). Facility-based experimental support was provided by MD Anderson Cancer Center Support Grant P30CA016672. X.L. was a recipient of the Idea Development Award-New Investigator (W81XWH-14-1-0576) from the Department of Defense Prostate Cancer Research Program (PCRP). X.L. is also a current recipient of the KL2 Young Investigator Award from Indiana Clinical and Translational Sciences Institute (CTSI), which is funded in part by grants KL2TR001106 and UL1TR001108 from the National Institutes of Health, National Center for Advancing Translational Sciences, Clinical and Translational Sciences Award.

References

Abeshouse A, Ahn J, Akbani R, Ally A, Amin S, Andry Christopher D, Annala M, Aprikian A, Armenia J, Arora A, et al. 2015. The molecular taxonomy of primary prostate cancer. *Cell* **163:** 1011–1025.

Barnes J, Anthony CT, Wall N, Steiner MS. 1995. Bone morphogenetic protein-6 expression in normal and malignant prostate. *World J Urol* **13:** 337–343.

Beppu H, Lei H, Bloch KD, Li E. 2005. Generation of a floxed allele of the mouse BMP type II receptor gene. *Genesis* **41:** 133–137.

Bjerke GA, Yang CS, Frierson HF, Paschal BM, Wotton D. 2014. Activation of Akt signaling in prostate induces a TGFβ-mediated restraint on cancer progression and metastasis. *Oncogene* **33:** 3660–3667.

Cai B, Chang SH, Becker EBE, Bonni A, Xia Z. 2006. p38 MAP kinase mediates apoptosis through phosphorylation of BimEL at Ser-65. *J Biol Chem* **281:** 25215–25222.

Chen Z, Trotman LC, Shaffer D, Lin H-K, Dotan ZA, Niki M, Koutcher JA, Scher HI, Ludwig T, Gerald W, et al. 2005. Crucial role of p53-dependent cellular senescence in suppression of Pten-deficient tumorigenesis. *Nature* **436:** 725–730.

Chua CW, Shibata M, Lei M, Toivanen R, Barlow LJ, Bergren SK, Badani KK, McKiernan JM, Benson MC, Hibshoosh H, et al. 2014. Single luminal epithelial progenitors can generate prostate organoids in culture. *Nat Cell Biol* **16:** 951–961.

Chytil A, Magnuson MA, Wright CV, Moses HL. 2002. Conditional inactivation of the TGF-β type II receptor using Cre:Lox. *Genesis* **32:** 73–75.

Darby S, Cross SS, Brown NJ, Hamdy FC, Robson CN. 2008. BMP-6 overexpression in prostate cancer is associated with increased Id-1 protein and a more invasive phenotype. *J Pathol* **214:** 394–404.

Ding Z, Wu C-J, Chu GC, Xiao Y, Ho D, Zhang J, Perry SR, Labrot ES, Wu X, Lis R, et al. 2011. SMAD4-dependent barrier constrains prostate cancer growth and metastatic progression. *Nature* **470:** 269–273.

Ding Z, Wu CJ, Jaskelioff M, Ivanova E, Kost-Alimova M, Protopopov A, Chu GC, Wang G, Lu X, Labrot ES, et al. 2012. Telomerase reactivation following telomere dysfunction yields murine prostate tumors with bone metastases. *Cell* **148:** 896–907.

Fournier PG, Juarez P, Jiang G, Clines GA, Niewolna M, Kim HS, Walton HW, Peng XH, Liu Y, Mohammad KS, et al. 2015. The TGF-β signaling regulator PMEPA1 suppresses prostate cancer metastases to bone. *Cancer Cell* **27:** 809–821.

Fujita M, Kohanbash G, Fellows-Mayle W, Hamilton RL, Komohara Y, Decker SA, Ohlfest JR, Okada H. 2011. COX-2 blockade suppresses gliomagenesis by inhibiting myeloid-derived suppressor cells. *Cancer Res* **71:** 2664–2674.

Gao H, Chakraborty G, Lee-Lim AP, Mo Q, Decker M, Vonica A, Shen R, Brogi E, Brivanlou AH, Giancotti FG. 2012. The BMP inhibitor Coco reactivates breast cancer cells at lung metastatic sites. *Cell* **150:** 764–779.

Garcia AJ, Ruscetti M, Arenzana TL, Tran LM, Bianci-Frias D, Sybert E, Priceman SJ, Wu L, Nelson PS, Smale ST, et al. 2014. Pten null prostate epithelium promotes localized myeloid-derived suppressor cell expansion and immune suppression during tumor initiation and progression. *Mol Cell Biol* **34:** 2017–2028.

Ilkovitch D, Carrio R, Lopez DM. 2012. uPA and uPA-receptor are involved in cancer-associated myeloid-derived suppressor cell accumulation. *Anticancer Res* **32:** 4263–4270.

Keller B, Yang T, Chen Y, Munivez E, Bertin T, Zabel B, Lee B. 2011. Interaction of TGFβ and BMP signaling pathways during chondrogenesis. *PLoS One* **6:** e16421.

Kobayashi A, Okuda H, Xing F, Pandey PR, Watabe M, Hirota S, Pai SK, Liu W, Fukuda K, Chambers C, et al. 2011. Bone morphogenetic protein 7 in dormancy and metastasis of prostate cancer stem-like cells in bone. *J Exp Med* **208:** 2641–2655.

Kwon SJ, Lee GT, Lee JH, Iwakura Y, Kim WJ, Kim IY. 2014. Mechanism of pro-tumorigenic effect of BMP-6: neovascularization involving tumor-associated macrophages and IL-1a. *Prostate* **74:** 121–133.

Lee YC, Cheng CJ, Bilen MA, Lu JF, Satcher RL, Yu-Lee LY, Gallick GE, Maity SN, Lin SH. 2011. BMP4 promotes prostate tumor growth in bone through osteogenesis. *Cancer Res* **71:** 5194–5203.

Li XL, Liu YB, Ma EG, Shen WX, Li H, Zhang YN. 2015. Synergistic effect of BMP9 and TGF-β in the proliferation and differentiation of osteoblasts. *Genet Mol Res* **14:** 7605–7615.

Lin SC, Lee YC, Yu G, Cheng CJ, Zhou X, Chu K, Murshed M, Le NT, Baseler L, Abe JI, et al. 2017. Endothelial-to-osteoblast conversion generates osteoblastic metastasis of prostate cancer. *Dev Cell* **41:** 467–480.e3.

Lu L, Ma J, Wang X, Wang J, Zhang F, Yu J, He G, Xu B, Brand DD, Horwitz DA, et al. 2010. Synergistic effect of TGF-β superfamily members on the induction of Foxp3+ Treg. *Eur J Immunol* **40:** 142–152.

Massagué J. 2008. TGFβ in cancer. *Cell* **134:** 215–230.

McDonnell MA, Law BK, Serra R, Moses HL. 2001. Antagonistic effects of TGFβ1 and BMP-6 on skin keratinocyte differentiation. *Exp Cell Res* **263:** 265–273.

Muzumdar MD, Tasic B, Miyamichi K, Li N, Luo L. 2007. A global double-fluorescent cre reporter mouse. *Genesis* **45:** 593–605.

Nguyen V, Meyers CA, Yan N, Agarwal S, Levi B, James AW. 2017. BMP-2-induced bone formation and neural inflammation. *J Orthop* **14:** 252–256.

Robinson D, Van Allen EM, Wu YM, Schultz N, Lonigro RJ, Mosquera JM, Montgomery B, Taplin ME, Pritchard CC, Attard G, et al. 2015. Integrative clinical genomics of advanced prostate cancer. *Cell* **161:** 1215–1228.

Scherner O, Meurer SK, Tihaa L, Gressner AM, Weiskirchen R. 2007. Endoglin differentially modulates antagonistic transforming growth factor-β1 and BMP-7 signaling. *J Biol Chem* **282:** 13934–13943.

Shen MM, Abate-Shen C. 2010. Molecular genetics of prostate cancer: new prospects for old challenges. *Genes Dev* **24:** 1967–2000.

Trotman LC, Niki M, Dotan ZA, Koutcher JA, Di Cristofano A, Xiao A, Khoo AS, Roy-Burman P, Greenberg NM, Dyke TV, et al. 2003. Pten dose dictates cancer progression in the prostate. *PLoS Biol* **1:** e59.

Wang S, Gao J, Lei Q, Rozengurt N, Pritchard C, Jiao J, Thomas GV, Li G, Roy-Burman P, Nelson PS, et al. 2003. Prostate-specific deletion of the murine Pten tumor suppressor gene leads to metastatic prostate cancer. *Cancer Cell* **4:** 209–221.

Wang G, Lu X, Dey P, Deng P, Wu CC, Jiang S, Fang Z, Zhao K, Konaparthi R, Hua S, et al. 2016. Targeting YAP-dependent MDSC infiltration impairs tumor progression. *Cancer Discov* **6:** 80–95.

Wood DP, Banks ER, Humphreys S, McRoberts JW, Rangnekar VM. 1994. Identification of bone marrow micrometastases in patients with prostate cancer. *Cancer* **74:** 2533–2540.

Yang S, Zhong C, Frenkel B, Reddi AH, Roy-Burman P. 2005. Diverse biological effect and Smad signaling of bone morphogenetic protein 7 in prostate tumor cells. *Cancer Res* **65:** 5769–5777.

Ye S, Yim JH, Kim JR, Jang KY, Wang H, Wang JC, Lee KB. 2015. Effects of diclofenac sodium on BMP-induced inflammation in a rodent model. *Spine* **40:** E799–E807.

Yuen HF, Chan YP, Cheung WL, Wong YC, Wang X, Chan KW. 2008. The prognostic significance of BMP-6 signaling in prostate cancer. *Mod Pathol* **21:** 1436–1443.

Zhang YE. 2009. Non-Smad pathways in TGF-β signaling. *Cell Res* **19:** 128–139.